

# A NO-REFERENCE IMAGE SHARPNESS ESTIMATION BASED ON EXPECTATION OF WAVELET TRANSFORM COEFFICIENTS

Hengjun Zhao<sup>\*‡</sup> Bin Fang<sup>\*\*</sup> Yuan Yan Tang<sup>†\*</sup>

<sup>\*</sup> Chongqing University, College of Computer and Science, Chongqing, China, 400030

<sup>†</sup> Macau University, Department of Computer and Information, Macau, China, 999078

<sup>‡</sup> Chongqing University of Arts and Sciences, Department of Mathematics & KLDAIP, China, 402160

## ABSTRACT

In this work, the expectation of wavelet transform coefficients is used for estimating an image sharpness. It's based on the observation that the greater the probability of big detail coefficients, the more pixels appear sharply, and consequently, the sharper the image. Specifically, an input image is firstly decomposed into three directional sub-bands by a separable discrete wavelet transform. Then these directional sub-bands are viewed as three random variables, and their expectations are computed. Finally, The proposed sharpness index is the weighted sum of three expectations. The experiments show that, despite its simplicity, the proposed sharpness index is competitive with the current best-performance techniques for no-reference image sharpness estimation.

**Index Terms**— image sharpness metric, expectation, wavelet decomposition

## 1. INTRODUCTION

Objective sharpness metrics have been used in many image processings and engineering applications including, for example, image quality assessment, main-subject detection [1], visual perception-based auto-focus cameras, and astigmatism correction in the scanning electron microscope [2]. Depending on how much information from the reference image is used, objective sharpness metrics can be divided into three types: full-reference, reduced-reference, and no-reference metrics. Full-reference metrics need full information of the reference image, and the reduced-reference metrics make use of a part of the information of the reference image. However, in many real-world scenarios, the reference image does not exist or is unavailable. Therefore, it is important to develop no-reference metrics that do not use any information about the reference image.

In the literature, a number of no-reference metrics have been developed. The easiest way to assess the sharpness of

an image is to calculate the variance of all image gray values [3]. It is based on the fact that when an image is blurred, the transitions between the gray levels decrease. As a result, the variance decreases. Another simple technique is to define sharpness metric based on histogram. Firestone *et al.* [4] defined their sharpness as the weighted sum of the histogram bins values above a certain threshold “ $T$ ”. The weights are set to the gray levels themselves, and the threshold, “ $T$ ”, is selected to be near the mean of the image. Based on the idea that entropy increases when the probability of occurrence of gray level decreases and vice versa, Chern *et al.* [5] defined a sharpness metric on the entropy computed from the histogram of the image gray values. Besides the above variance and histogram, the kurtosis, a statistical measure of the peakedness and flatness of a distribution, is also used to measure image's sharpness. For example, Zhang *et al.* [6] estimated the sharpness based on the kurtosis of the power spectral density of the image. Using the discrete cosine transform (DCT), Caviedes *et al.* [7] built a block-based sharpness estimator using the kurtosis of DCT coefficients of each block. And the overall sharpness estimation is given by the average of the sharpness values computed for edge profiles.

From the observation that a blurred image has wider edges, many no-reference metrics involve measuring the spread of edge. Marziliano *et al.* [8] first identified vertical edges in an image, and then estimated overall sharpness based on the average edge width. Ong *et al.* [9] determined the image sharpness as the average extent in both the gradient direction and the opposite direction of edges in the image. Ferzli *et al.* [10] presented a perceptual-based no-reference objective image sharpness metric by integrating the concept of Just Noticeable Blur (JNB) into a probability summation model. The JNB is the minimum amount of perceived blur-iness around an edge given a contrast higher than the “just noticeable difference” [11]. Using the concept of JNB in a different way, Narvekar *et al.* [12] estimated the sharpness of an image as the cumulative probability of detecting blur in an image.

It is well known that the attenuation of high-frequency content leads to an image that appears blurred. Hence vari-

<sup>\*</sup>This material is based on work supported by, or in part by, the Fundamental Research Funds for the Central University (CDJXS11182240) and the National Natural Science Foundation of China (61173129, 61173130, 61273244, 61271452, 61100114).

ous DCT, discrete wavelet transform (DWT), and other transforms have also been used to detect the image's sharpness. Ferzli *et al.* [13] applied the dyadic wavelet transform to the image and then measured the kurtosis of the two-dimensional discrete fourier transform of the wavelet coefficients across large scales. Hassen *et al.* [14] proposed a sharpness metric based on the local phase coherence measured via complex wavelets. Vu *et al.* [15] presented a fast image sharpness (FISH) based on a three-level discrete wavelet transform (DWT) for estimating both global and local image sharpness, which operates under the assumption that the perceived sharpness could be estimated by examining the log-energy of the DWT high-frequency bands. Based on the local maximum total variation and the slope of the local magnitude spectrum, Vu *et al.* [16] proposed an algorithm that can measure the perceived sharpness of local image and global image.

In the wavelet theory, the magnitude of detail coefficient at some pixel indirectly represents the gray value variation between this pixel and its neighbor. The larger the magnitude of detail coefficient, the larger the gray value variation, and consequently, the sharper the pixel. Hence, the sum of magnitude of all detail coefficients can indicate the global image sharpness. However, this sum metric is not always accurate because of different image size and the randomness of image contents. On the other side, just because of the randomness of image contents, detail coefficients can be viewed as values of a random variable. And, the greater the probability of big detail coefficient, the more pixels appear sharply, and consequently, the sharper the global image. Therefore, we use the expectation of detail sub-bands to measure the image sharpness in this work.

This work is organized as follows. Section II presents the detail of the proposed sharpness index. Experimental results are given in section III. General conclusions are given in section IV.

## 2. SHARPNESS BASED ON EXPECTATION

### 2.1. Global Sharpness

Given a gray scale input image  $I$ , the proposed global sharpness index is computed by the following three steps.

1) *Decompose the input image.* The gray-scale input image is decomposed into three directional detail sub-bands by a wavelet transform filter. Let  $S_{HD}(i)$ ,  $S_{VD}(i)$  and  $S_{DD}(i)$  denote the absolute value of the horizontal detail (HD) coefficient, the vertical detail (VD) coefficient, and the diagonal detail (DD) coefficient, respectively. And  $i = 1, \dots, L$ , where  $L = \frac{R}{2} \times \frac{C}{2}$ ,  $R$  and  $C$  are the numbers of the row and the column of the input image, respectively.

2) *Compute the expectation of each detail sub-band.* When observing two images, the image that appears sharper is not necessarily one that contains more sharp regions. Instead, visual summation dictates that the sharpness

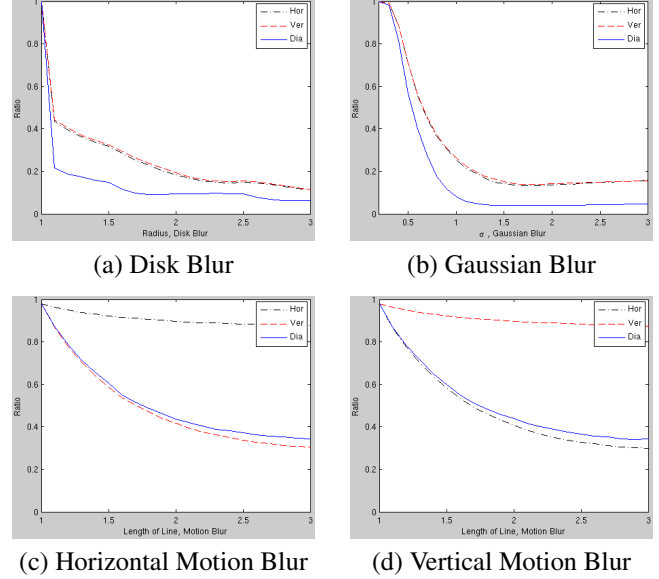


**Fig. 1.** The performance of three directional sub-bands' expectation when original image is blurred by different PSFs. (Horizontal sub-band: Black dash-dot line; Vertical sub-band: Red dashed line; and Diagonal sub-band: Blue line.)

is determined based on the sharpest regions in each image [16]. In other words, the small detail coefficients which account for a large proportion of all detail coefficients make a little contribution to the image sharpness. Therefore, we only use the  $T\%$  of the largest elements of each detail sub-band to construct an accurate sharpness metric. In our experiments to test the global image sharpness, the  $T\%$  is set to 1%.

Let  $\{\widehat{S}_{XY}(i)\}_{i=1}^M$  be the vector consisting of the first  $M$  elements of the sorted vector  $\widetilde{S}_{XY}$  in descending order as  $\widetilde{S}_{XY} = \text{sort}_d(S_{XY}(i))$ , where  $M = \lfloor L \times T\% \rfloor$  is the number of elements in the subset containing  $T\%$  of the largest values of  $S_{XY}(i)$ , and  $XY$  is either  $HD$ ,  $VD$  or  $DD$ . To calculate the expectation of  $XY$  sub-band, we firstly divide the vector  $\{\widehat{S}_{XY}(i)\}_{i=1}^M$  into  $N$  equally spaced bins, where  $N$  given by  $N = \lceil \widetilde{S}_{XY}(1)/20 \rceil$  is the number of bins. Consequently, we get two vectors  $\{C(i)\}_{i=1}^N$  and  $\{L(i)\}_{i=1}^N$  containing the frequency counts and the bin locations. Next, we calculate the expectation of  $XY$  sub-band via

$$E_{XY} = \sum_{i=1}^N L(i) \frac{C(i)}{M}. \quad (1)$$

3) *Compute the sharpness index.* Finally, the image's overall sharpness index is given as follows:

$$\text{Sharpness} = \sqrt{\alpha E_{HD} + \beta E_{VD} + \gamma E_{DD}}. \quad (2)$$

where  $\alpha$ ,  $\beta$  and  $\gamma$  are the weights, and  $\alpha + \beta + \gamma = 1$ .

The de-focused blur and linear motion blur are two famous and frequent image blurs. And they can be expressed using a standard linear convolution model as  $g(x, y) = f(x, y) * h(x, y)$ , where  $g(x, y)$  denotes the blur image,  $f(x, y)$  denotes the ideal image, and  $h(x, y)$  denotes the space-invariant point spread function (PSF) with  $*$  as a two-dimensional linear convolution process. Fig.1 shows the performance of horizontal sub-band's expectation (black dash-dot line), vertical sub-band's expectation (red dashed line) and diagonal sub-band's expectation (blue line) when the original image is blurred by different PSFs. The *Y axis Ratio* is the ratio of the blurred image sub-band's expectation to the original image sub-band's expectation. And the tested images in Fig.1.(a), Fig.1.(b), Fig.1.(c) and Fig.1.(d) are blurred by the disk PSF with radius from 1 to 3, the Gaussian PSF with  $\sigma$  from 0.3 to 3, the horizontal motion PSF with length from 1 to 3 and the vertical motion PSF with length from 1 to 3, respectively. From Fig.1, we can easily note that the diagonal sub-band's expectation is more sensitive to the blurriness than the horizontal and vertical sub-band's expectation. Hence, the  $\alpha$ ,  $\beta$  and  $\gamma$  are set to 0.2, 0.2 and 0.6, respectively, in our experiment section.

## 2.2. Sharpness Map

In this subsection, we apply the global sharpness to small blocks of the entire image, and generate a sharpness map.

To generate the sharpness map, the entire image is firstly divided into small blocks of size  $10 \times 10$  with 50% overlap between two consecutive blocks. Next, the global sharpness described in previous subsection is applied to each image block. Because the block is very small related to whole image, the parameter  $T\%$  is set to 100% in the block's sharpness index with the aim of generating an accurate sharpness. Fig.2 shows six sharpness maps generated by this process.

With the same approach used in  $S_3$  [16] and FISH [15], it is also possible to collapse the sharpness map into a scalar sharpness index representing the image's overall sharpness. That is

$$Sharpness_{bb} = \sqrt{\frac{1}{k} \sum_{i=1}^k Sharpness^2(i)} \quad (3)$$

where  $k$  denotes the number of block which receives the 1% largest local sharpness of sharpness map. The value 1% is used because the overall perceived sharpness of an image is largely determined by the image's sharpest regions.

## 3. EXPERIMENTAL RESULTS

In this section, we firstly demonstrate that the proposed Expectation-based Sharpness ( $EBS$ ) and Block-based  $EBS$  ( $EBS_{bb}$ ) can accurately estimate across-image and within-image sharpness, respectively. Next, we demonstrate the

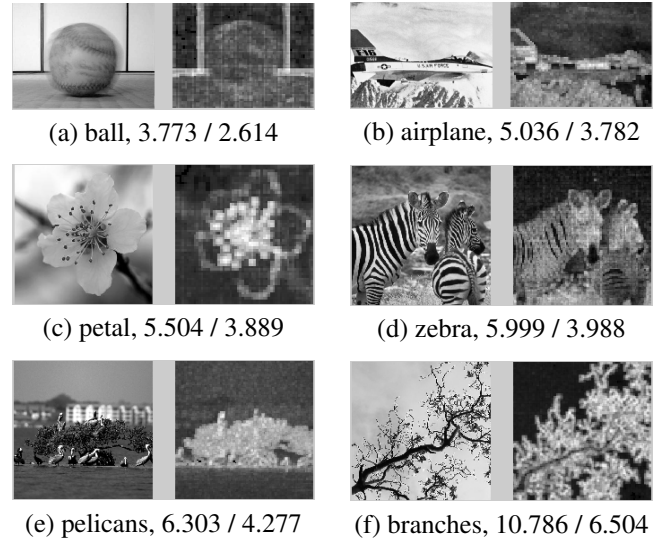


**Fig. 2.** Representative maps generated by using  $EBS_{bb}$  along with sharpness indices computed via  $EBS / EBS_{bb}$ . The images were organized in the order to overall sharpness judged by human subjects [16].

utility of proposed sharpness index on no-reference quality assessment of blurred images from four image-quality database. The wavelet filter used in our experiments is the Daubechies 7 (db7) [17] filter.

### 3.1. Representative Results

Fig.2 depicts the  $EBS_{bb}$  maps and sharpness indices estimated by  $EBS$  and  $EBS_{bb}$ . The images in this figure are from S3[16] web-page and ordered based on subjective ratings of sharpness [16].

In terms of across-image prediction, the  $EBS$  and  $EBS_{bb}$  indices agree with the relative perceive sharpness across these image. For example, the blur image *ball* gets the lowest  $EBS / EBS_{bb}$  indices; The image *branches*, which contains very sharp tree branches, gets the greatest  $EBS$  and  $EBS_{bb}$  indices.

In terms of within-image sharpness,  $EBS_{bb}$  map quite accurately captures the sharpness regions in each image. For example, in image *ball*, the ball is blurry, and this region is dark in the corresponding  $EBS_{bb}$  map. The branches in image *branches* are much sharper than the sky; This fact is also reflected in the corresponding  $EBS_{bb}$

### 3.2. No-Reference Quality Assessment of Blurred Images

To analysis the performance of  $EBS$  and  $EBS_{bb}$  indices, we employ the blur image subsets of four publicly available image databases: 1) the CSIQ database[18] (containing 150 blurred images); 2) the LIVE2 database[19] (145 blurred images); 3) the TID database[20] (96 blurred images); and 4)

	CSIQ	LIVE2	TID	IVC	Avg.	W. Avg.
CC						
JNBM	0.806	0.816	0.727	0.698	0.762	0.786
CPBD	0.882	0.896	0.848	0.801	0.857	0.875
BLIINDS-II	0.893	0.893	0.737	0.781	0.826	0.851
S3	0.911	0.944	<b>0.874</b>	0.927	0.914	0.915
FISH	0.923	0.91	0.816	<b>0.957</b>	0.902	0.895
FISH <sub>bb</sub>	<b>0.943</b>	<b>0.944</b>	<b>0.858</b>	0.941	<b>0.922</b>	<b>0.923</b>
EBS	0.903	0.927	0.841	0.949	0.905	0.899
EBS <sub>bb</sub>	<b>0.948</b>	<b>0.945</b>	0.842	<b>0.963</b>	<b>0.925</b>	<b>0.923</b>
SROCC						
JNBM	0.762	0.786	0.714	0.666	0.732	0.755
CPBD	0.886	0.92	<b>0.854</b>	0.769	0.857	0.885
BLIINDS-II	0.877	0.894	0.794	0.527	0.773	0.847
S3	0.906	<b>0.944</b>	<b>0.85</b>	0.869	0.892	<b>0.905</b>
FISH	0.894	0.886	0.787	<b>0.932</b>	0.875	0.895
FISH <sub>bb</sub>	<b>0.917</b>	<b>0.938</b>	0.841	0.919	<b>0.904</b>	<b>0.907</b>
EBS	0.901	0.912	0.829	0.906	0.887	0.888
EBS <sub>bb</sub>	<b>0.918</b>	0.932	0.827	<b>0.954</b>	<b>0.908</b>	0.903
OR						
JNBM	36.67%	13.79%	72.92%		41.13%	37.09%
CPBD	37.67%	8.28%	68.75%		37.9%	34.02%
BLIINDS-II	30.67%	10.34%	80.21%		40.41%	35.29%
S3	32.67%	1.38%	67.72%		33.92%	29.67%
FISH	26.00%	3.45%	<b>66.67%</b>		32.04%	27.62%
FISH <sub>bb</sub>	<b>24.00%</b>	<b>0.8%</b>	70.4%		<b>31.73%</b>	<b>26.79%</b>
EBS	34.00%	3.45%	<b>67.71%</b>		35.05%	30.94%
EBS <sub>bb</sub>	<b>20.70%</b>	<b>0.7%</b>	68.8%		<b>30.07%</b>	<b>25.09%</b>
OD						
JNBM	6.285	101.597	39.421		49.101	49.767
CPBD	4.272	58.853	<b>27.316</b>		30.147	30.171
BLIINDS-II	3.759	50.494	41.629		31.961	30.388
S3	3.037	1.807	<b>23.42</b>		<b>9.421</b>	<b>7.585</b>
FISH	2.425	7.014	32.107		13.849	11.414
FISH <sub>bb</sub>	<b>1.658</b>	<b>1.048</b>	28.315		10.34	7.977
EBS	3.531	8.629	28.585		13.582	11.573
EBS <sub>bb</sub>	<b>1.321</b>	<b>1.583</b>	27.896		<b>10.267</b>	<b>7.943</b>

**Table 1.** Performances of various algorithms on the blurred images from the CSIQ, LIVE2, TID and IVC databases. “W. Avg.” is the average weighted by number of images in each database. The EBS and EBS<sub>bb</sub> are the proposed indices.

the IVC database[21] (20 blurred images). And all color images are converted into gray-scale images. The CSIQ and TID releases the standard deviations of the DMOS and MOS, respectively. However the LIVE2 and IVC do not release the standard deviations. It is necessary to note that the standard deviations of DMOS for each blurred image in LIVE2, are from the CPBD software. We compared our sharpness indices against five sharpness estimator (*JNBM*[10], *CPBD*[22], *S3*[16], *FISH* and *FISH<sub>bb</sub>*[15]), and one no-reference image quality estimator (*BLIINDS – II*[23]). We list the URLs of four databased and four softwares in Appendix section. The performance is measured in terms of : 1) Pearson correlation coefficient (CC); 2) Spearman rank-order correlation (SROCC); 3) Outlier Ratio (OR); and 4) Outlier distance (OD).

Table 1 summarizes the performance of *EBS*, *EBS<sub>bb</sub>* and other algorithms on this evaluation. A sharpness estimator aims to simultaneously obtain high CC and SROCC, and low OR and OD. The two best results are highlighted in this table. Note that the OR and OD are not calculated on IVC because the standard deviations between subjects have not been released for this database. In generally, the *EBS* and *EBS<sub>bb</sub>*

perform well on all four databases on almost all criteria. In terms of CC, OR and OD, *EBS<sub>bb</sub>* outperforms other methods on the two databases (CSIQ and LIVE2) and is competitive on the other two databases. When compared to the similar sharpness index *FISH*, the *EBS* is better than *FISH* in terms of SROCC on three big databases: CSIQ, LIVE2 and TID. The *EBS* values of “Avg.” and “W. Avg.” in terms of SROCC and CC are both bigger than *FISH* values.

#### 4. CONCLUSION

In this work, we propose a new index for estimating global image sharpness, which operates by first decomposing the input image via a separable DWT, and then estimating sharpness based on a weighted geometric mean of each DWT sub-band expectation. By applying the same computation to small image block, we generate a local sharpness map. The effectiveness of proposed sharpness index on four image databases is also presented.

### Appendix: The URL of used Softwares and Databases

#### Softwares

JNBM[10]: <http://ivulab.asu.edu/software/jnbnm>  
 CPBD[22]: <http://ivulab.asu.edu/software/cpbd-better-than-jnbnm>  
 BLIIND-II[23]: <http://live.ece.utexas.edu/research/quality>  
 S3[16]: <http://vision.okstate.edu/s3/>

#### DataBase

CSIQ[18]: <http://vision.okstate.edu/?loc=csiq>  
 LIVE2[19]: <http://live.ece.utexas.edu/research/quality/>  
 TID[20]: <http://www.ponomarenko.info/tid2008.htm>  
 IVC[21]: <http://www2.irccyn.ec-nantes.fr/ivcdb/>

#### 5. REFERENCES

- [1] C. Vu and D. Chandler, “Main subject detection via adaptive feature refinement,” *Journal of Electronic Imaging*, vol. 20, no. 1, pp. 013011–013011, 2011.
- [2] CF Batten, DM Holburn, BC Breton, and NHM Caldwell, “Sharpness search algorithms for automatic focusing in the scanning electron microscope,” *Scanning*, vol. 23, no. 2, pp. 112–113, 2001.
- [3] SJ Erasmus and KCA Smith, “An automatic focusing and astigmatism correction system for the sem and ctem,” *Journal of Microscopy*, vol. 127, no. 2, pp. 185–199, 1982.

- [4] L. Firestone, K. Cook, K. Culp, N. Talsania, K. Preston Jr, et al., "Comparison of autofocus methods for automated microscopy," *Cytometry*, vol. 12, no. 3, pp. 195, 1991.
- [5] N. Ng Kuang Chern, P.A. Neow, and M.H. Ang Jr, "Practical issues in pixel-based autofocusing for machine vision," in *Robotics and Automation, 2001. Proceedings 2001 ICRA. IEEE International Conference on*. IEEE, 2001, vol. 3, pp. 2791–2796.
- [6] N. Zhang, A. Vladar, and B. Larrabee, "A kurtosis-based statistical measure for two-dimensional processes and its applications to image sharpness," in *Proceedings of the 2003 Section on Physical and Engineering Sciences*, 2003, pp. 4730–4736.
- [7] J. Caviedes and S. Gurbuz, "No-reference sharpness metric based on local edge kurtosis," in *Image Processing, 2002. Proceedings. 2002 International Conference on*. IEEE, 2002, vol. 3, pp. III–53.
- [8] P. Marziliano, F. Dufaux, S. Winkler, and T. Ebrahimi, "A no-reference perceptual blur metric," in *Image Processing, 2002. Proceedings. 2002 International Conference on*. IEEE, 2002, vol. 3, pp. III–57.
- [9] E. Ong, W. Lin, Z. Lu, X. Yang, S. Yao, F. Pan, L. Jiang, and F. Moschetti, "A no-reference quality metric for measuring image blur," in *Signal Processing and Its Applications, 2003. Proceedings. Seventh International Symposium on*. IEEE, 2003, vol. 1, pp. 469–472.
- [10] R. Ferzli and L.J. Karam, "A no-reference objective image sharpness metric based on the notion of just noticeable blur (jnb)," *Image Processing, IEEE Transactions on*, vol. 18, no. 4, pp. 717–728, 2009.
- [11] N. Jayant, J. Johnston, and R. Safranek, "Signal compression based on models of human perception," *Proceedings of the IEEE*, vol. 81, no. 10, pp. 1385–1422, 1993.
- [12] N.D. Narvekar and L.J. Karam, "A no-reference perceptual image sharpness metric based on a cumulative probability of blur detection," in *Quality of Multimedia Experience, 2009. QoMEX 2009. International Workshop on*. IEEE, 2009, pp. 87–91.
- [13] R. Ferzli, L.J. Karam, and J. Caviedes, "A robust image sharpness metric based on kurtosis measurement of wavelet coefficients," in *Proc. of Int. Workshop on Video Processing and Quality Metrics for Consumer Electronics*, 2005.
- [14] R. Hassen, Z. Wang, and M. Salama, "No-reference image sharpness assessment based on local phase coherence measurement," in *Acoustics Speech and Signal Processing (ICASSP), 2010 IEEE International Conference on*. IEEE, 2010, pp. 2434–2437.
- [15] P.V. Vu and D.M. Chandler, "A fast wavelet-based algorithm for global and local image sharpness estimation," *Signal Processing Letters, IEEE*, vol. 19, no. 7, pp. 423–426, 2012.
- [16] C.T. Vu, T.D. Phan, and D.M. Chandler, "S3: A spectral and spatial measure of local perceived sharpness in natural images," *IEEE Transactions on Image Processing*, vol. 21, no. 3, pp. 934, 2012.
- [17] I. Daubechies et al., *Ten lectures on wavelets*, vol. 61, SIAM, 1992.
- [18] Eric C. Larson and Damon M. Chandler, "Most apparent distortion: full-reference image quality assessment and the role of strategy," *Journal of Electronic Imaging*, vol. 19, no. 1, pp. 011006, 2010.
- [19] H.R. Sheikh, M.F. Sabir, and A.C. Bovik, "A statistical evaluation of recent full reference image quality assessment algorithms," *Image Processing, IEEE Transactions on*, vol. 15, no. 11, pp. 3440–3451, 2006.
- [20] N. Ponomarenko, V. Lukin, A. Zelensky, K. Egiazarian, M. Carli, and F. Battisti, "Tid2008-a database for evaluation of full-reference visual quality assessment metrics," *Advances of Modern Radioelectronics*, vol. 10, no. 10, pp. 30–45, 2009.
- [21] A. Ninassi, P. Le Callet, and F. Atrousseau, "Pseudo no reference image quality metric using perceptual data hiding," in *Proceedings of SPIE*, 2006, vol. 6057, pp. 146–157.
- [22] N.D. Narvekar and L.J. Karam, "A no-reference image blur metric based on the cumulative probability of blur detection (cpbd)," *Image Processing, IEEE Transactions on*, vol. 20, no. 9, pp. 2678–2683, 2011.
- [23] M.A. Saad, A.C. Bovik, and C. Charrier, "Blind image quality assessment: A natural scene statistics approach in the dct domain," *Image Processing, IEEE Transactions on*, vol. 21, no. 8, pp. 3339–3352, 2012.